Submitted to
IEEE Trans. on Nuclear Science

LBL-2035
Preprint c. 1

NANOSECOND PULSE AMPLIFIERS

H. G. Jackson

July 1973

Prepared for the U.S. Atomic Energy Commission
under Contract W-7405-ENG-48

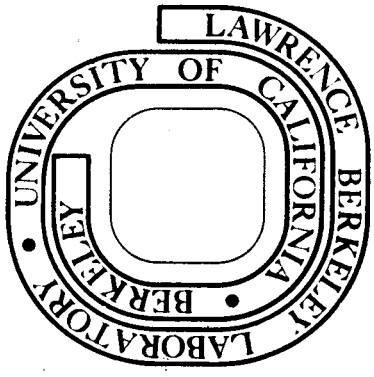

LBL-2035

DISCLAIMER

NANOSECOND PULSE AMPLIFIERS*

H. G. Jackson

Lawrence Berkeley Laboratory
University of California
Berkeley, California 94720

SUMMARY

Examples are given of the use of pulse amplifiers in three areas of experimental nuclear physics. The necessity of low noise at the input of these amplifiers leads to a discussion of electronic noise. The need for pulse-shaping networks in amplifiers particularly designed for accurate amplitude analysis is emphasized.

The technique of using negative feedback to obtain nanosecond pulse amplifiers is discussed. Calculated and experimental results are given for two series-shunt feedback pair amplifiers. The necessity of using the hybrid fabrication technique in subnanosecond pulse amplifiers is shown as well as the characterization of the transistors and complete amplifier with the scattering (s) parameters.

An annotated bibliography is included as an appendix.

INTRODUCTION

High-speed pulse amplifiers are widely used in amplitude and time analysis measurements in experimental nuclear physics. We first consider three specific examples of nuclear physics instrumentation taken from i) high-, ii) medium-, iii) low-energy physics research.

High-Energy Physics Example

In Fig. 1 we show a block diagram of a simple high-energy nuclear physics instrumentation system used in angular correlation studies. Here the particles in the beam are travelling at the speed of light (in one nanosecond they will have travelled about 30 cms). They are sufficiently energetic that they are capable of passing through the radiation detectors. However, their passage through the detector gives rise to an electrical pulse which is then amplified before being fed to an amplitude discriminator. From the discriminator we obtain a unit pulse (of fixed amplitude and time duration) for each incoming pulse that is above a predetermined amplitude threshold level. The coincidence circuit gives a unit output pulse if the two input pulses are in time coincidence. In our simple block diagram an event in counter #1 is indicative of a reaction in the target in which a secondary particle was formed and emitted from the target at an angle of +30° from the beam line. Similarly an event in counter #3 indicates a reaction with an angular displacement of -30°. An event in counter #2 indicates a secondary with no angular displacement or perhaps no secondary particle was formed. In this system we have been simply detecting the presence of a charged particle, indicated by a TRUE STATE or LOGIC ONE at the output of the discriminator.

Medium Energy Physics Example

The second example is typical of a medium energy physics experiment. In Fig. 2 we note that the particles in the beam are again sufficiently energetic that they pass through the radiation detectors. At the time a charged particle passes through detector D1 an electrical pulse is obtained from the detector. This pulse is connected to an amplifier and discriminator for the same purpose as in the previous example. The unit pulse from the discriminator is connected to the START input of a time analyzer. In similar fashion, the time the particle passes through detector D2 is indicated by a unit pulse applied to the STOP input of the time analyzer. The time analyzer gives us a measurement of the time interval between the START and STOP pulses. Hence, if the distance between the two detectors, D1 and D2 is known, we have a measurement of the velocity of the particles in the beam. From this time-of-flight measurement we can determine the energy and mass of the charged particles.

Low Energy Physics Example

The final example in nuclear physics instrumentation is taken from the low energy area. In Fig. 3 the range of the particles is sufficiently short that they are totally absorbed in the detector. The intention here is to measure the energy of the particles. Now the amplitude of the electrical pulse from the detector is directly proportional to the energy. (The range of the particles is also directly proportional to energy.) After amplification the pulses are usually fed to a pulse height analyzer. However, for our purposes here we can represent the pulse height analyzer as an analog-to-digital converter. The purpose of the ADC is to produce a digital code directly related to the amplitude of the incoming voltage signal. The digital code is then printed or otherwise displayed so that we may have a visual indication of the energy of the nuclear particles.

In each of these examples a nuclear particle interacts with the material of a radiation detector to produce, at the output of the detector, a small pulse of current (which may be less than 1 μA) with a fast leading edge (risetime of ~1 ns) and exponential trailing edge. These small pulses must generally be amplified before anything else can be done with them.

The accuracy with which the amplitude and time measurements can be made is limited by i) the statistical fluctuation of the detection process and ii) the electronic noise in the instrumentation system. Of

* This work was done under the auspices of the United States Atomic Energy Commission.

particular interest is the noise associated with the pulse amplifier. Attempting to measure a 1 μA pulse of current to an accuracy of 0.1% requires that the electronic noise in the system, when referred to the input of the amplifier, must be less than 1 nA. It is therefore appropriate for us to give some consideration to the problem of noise in pulse amplifiers.

NOISE

The electronic noise we are going to consider is due to the random fluctuations of current and voltage present in a circuit arising from the electronic components themselves. That is we will not be concerned with man-made electrical interference like pick-up from radio and TV stations.

The three main sources of electronic noise are thermal noise, shot noise and flicker noise.[1,2]

Thermal Noise

Thermal noise is associated with any resistive element and is the result of the random thermal motion of electrons in the conducting material. These electrons are in motion even if no electrical excitation is present. The average value of the motion of the electron is of course zero, but the rms (root mean square) value of the motion is finite.

We can represent the thermal noise in a resistor as a rms voltage in series with a noiseless resistor as in Fig. 4. Hence, the mean square value of the noise is given by

$$v_n^2 = 4\,kT\,R\,\Delta f$$

where k = Boltzmann constant $\left((1.38)\ (10^{-23})\right)$

T = temperature is °K

Δf = bandwidth, the range of frequency of interest.

The spectral density of thermal noise is flat with frequency, hence, thermal noise is known as "white" noise. It is also sometimes referred to as "Johnson noise", named after an early pioneer who studied this noise phenomenon in the later 1920's.

Shot Noise

Since the emission of electrons and holes across a pn junction is random in nature, we also have a noise source associated with a semiconductor junction diode. This is shot noise and from an analysis of the noise we have

$$i_n^2 = 2\,q\,I\,\Delta f$$

where q = electronic charge $\left((1.6)\ (10^{-19})\right)$

I = dc value of the current

Δf = bandwidth

Like thermal noise, the spectral density of shot noise is also flat with frequency.

In Fig. 5a we show a simple circuit of a battery V producing a current through the series circuit consisting of a diode and a resistor. In Fig. 5b we show a model for the noise components of this circuit. Notice that due to the randomness of the sources of noise, they are totally uncorrelated. Hence, to determine the total noise current in the circuit we sum the individual components of noise in quadrature. That is,

$$i_n^2 = i_{ns}^2 + i_{nt}^2$$

Flicker Noise

Most electronic devices produce an electrical noise called flicker noise which is important only at the very low frequencies. The spectral density of flicker noise varies inversely with frequency. Consequently this type of noise is often referred to as "1/f noise".

The origin of this noise is not well understood. But for a transistor the noise is certainly dependent on the surface treatment as well as the crystal imperfections of the device. In most present day devices flicker noise is only important in amplifiers at frequencies less than 1 KHz. As such, we are no longer interested in flicker noise in our presentation here.

Noise in BJT

Noise in a well designed pulse amplifier is due to the input stage only. However, all sources of noise in the amplifier can be combined and referred to the input of a noiseless amplifier, as in Fig. 6. Assuming the input stage to be a bipolar junction transistor (BJT) it is necessary to identify the sources of noise in this device. Figure 7 shows the small-signal hybrid-π model of the BJT, including the noise sources. The only thermal noise shown (v_{nb}) is due to the random motion of electrons in the ohmic base region of the transistor. Recombination of the minority carriers in the base is also a random process. Hence the base current is modeled as a source of shot noise, (i_{nb}). The collection of minority carriers at the collector-base junction is an independent random process. Therefore, the collector current is another source of shot noise, (i_{nc}). Hence we have the three following sources of noise in the BJT,

$$v_{nb}^2 = 4\,k\,T\,r_x\,\Delta f$$

$$i_{nb}^2 = 2\,q\,I_B\,\Delta f$$

$$i_{nc}^2 = 2\,q\,I_C\,\Delta f$$

To obtain an equivalent input noise voltage source, v_n, we can reflect the effect of the collector current noise back to the input if we recall that for the BJT,

$$v_\pi = \frac{i_c}{g_m}$$

$$\text{then } v_n^2 = v_{nb}^2 + \frac{i_{nc}^2}{g_m^2}$$

$$= 4\,k\,T\,r_x\,\Delta f + \frac{2\,q\,I_C\,\Delta f}{g_m^2}$$

$$= 4\,k\,T\left(r_x + \frac{1}{2\,g_m}\right)\Delta f$$

If we let $R_{eq} = \left(r_x + \frac{1}{2\,g_m}\right)$, we have an "equivalent input noise resistance". That is v_n^2 can be represented as the thermal noise of an equivalent resistor R_{eq}. (Since g_m is directly related to I_C we see that, except for very low operating currents, the effect of r_x is dominant). If we wish to refer to the noise current at the input we have

$$i_n^2 = i_{nb}^2 + \frac{i_{nc}^2}{|\beta_{(j\omega)}|^2}$$

where we have included $\beta_{(j\omega)}$ to account for the frequency dependence of β_o. Then,

$$i_n^2 = 2\,q\left(I_B + \frac{I_C}{|\beta_{(j\omega)}|^2}\right)\Delta f$$

Hence we now have an "equivalent input noise current".

$$I_{eq} = I_B + \frac{I_C}{|\beta_{(j\omega)}|^2}$$

Noise in FET

The noise in a field effect transistor (FET) is not due to shot noise since there are no junctions over which random current flow can occur. However, the channel material is necessarily resistive and gives rise to output noise.

A circuit model for the FET including the noise sources is shown in Fig. 8. For the FET,

$$i_{ng}^2 = 2\,q\,I_G\,\Delta f$$

$$i_{nd}^2 = 4\,K\,T\,\frac{0.7}{g_m}\,\Delta f$$

where, i_{ng} is the shot noise due to the gate leakage current. This is usually negligible unless the signal source resistance is very large ($\sim 10^{12}\ \Omega$). i_{nd} is the thermal noise due to the channel material. Notice, for the usual case, the equivalent input noise resistance is given by

$$R_{eq} = \frac{0.7}{g_m}$$

$$\text{then } v_n^2 = 4\,K\,T\,R_{eq}\,\Delta f$$

An important point to notice from the discussion of electronic noise is that both thermal noise and shot noise increase with bandwidth. Therefore for accurate amplitude analysis measurements it is advantageous to use both high and low frequency filters in the amplifier. Though in pulse amplifiers these filters are usually referred to as differentiating and integrating networks respectively, or just simply pulse shaping circuits. Generally, however, in a pulse amplifier designed for amplitude analysis there is one dominant differentiating time constant which is made equal to one dominant integrating time constant.[3] All other differentiating time constants are made very long and it is hoped all other integrating time constants are very short. A typical result of this type of pulse shaping in an amplifier used with a semiconductor radiation detector is shown in Fig. 9, where we show the noise in the amplifier as a function of two equal dominant time constants. We show the mean square value of the noise, in volts, referred to the input of the amplifier. Notice the noise is at a minimum when the equal time constants are ~1.0 μs. The center frequency of the bandpass of such an amplifier is about 160 kHz. Hence for amplitude analysis a relatively low frequency, narrow bandpass amplifier may be desired.

Another criterion that might be of interest is the pulse repetition rate. To do accurate amplitude analysis with an amplifier that has an upper cut-off frequency of 160 kHz, the pulse repetition rate must be less than 100 K pulses/sec. With higher repetition rates than this shorter differentiating and integrating time constants then 1.0 μs must be used, with a consequent increase in noise level and reduced accuracy.

WIDEBAND AMPLIFIERS

Our first two examples of nuclear physics instrumentation--the coincidence experiment and the time-of-flight experiment--require fast amplifiers so as not to introduce a large error in the timing of the nuclear particle through the radiation detector. The primary function of the fast amplifier is to amplify the signal from the detector without significantly degrading the risetime. Implicit in this statement is the fact that the upper cut-off frequency (f_h) of the amplifier is high since for many amplifier designs,

$$f_h = \frac{0.35}{t_r}$$

where t_r is the risetime (10 to 90%) of the output response to a step input.

Also to prevent shift of the amplifier operating conditions with high repetition rates it is desired that the lower cut-off frequency (f_l) be as low as possible. Ideally then, it is required that the bandwidth of the amplifier be very wide, from dc to as high as possible.

Negative Feedback

The technique of negative feedback allows us to exchange gain in an amplifier for bandwidth.[1,2] A typical gain frequency response of a high frequency transistor is shown in Fig. 10.

For a bandwidth of 10 MHz the current gain is 100 (i.e., 40 dB). To extend the bandwidth to 300 MHz requires that the gain of the transistor be reduced to 3.3. Two such stages of amplification would yield an overall gain of ~10 with a risetime of ~1.2 ns.

In applying negative feedback to a single stage of amplification there are two choices.

i) Series feedback, by connecting a resistor in series with the emitter of a common-emitter stage (Fig. 11a).

ii) Shunt feedback, by connecting a resistor in shunt from the collector to the base of a common-emitter stage (Fig. 11b).

Now it can be seen that the effect of the series feedback resistor is to increase the input resistance of the stage. It can also be shown that the effect of the shunt feedback resistor is to decrease the input resistance of the stage.

Now when the input signal to an amplifier is obtained from a voltage source it is obvious we require a high input resistance for the amplifier. Therefore series feedback is desired at the input of this amplifier. In similar fashion a low input resistance is indicated when the signal is obtained from a current source. Shunt feedback around the input transistor would be used in this case.

Common to many high-speed pulse systems is the 50-Ω transmission line which must be terminated in its characteristic impedance. Also, since the output from the collector of a transistor can easily be modeled as a current source, it follows that an optimum configuration of two transistors in a wideband amplifier application is the series-shunt cascade (Fig. 11c).

A minor disadvantage to this connection is that since the feedback is applied to each stage indivdually the overall gain is somewhat sensitive to parameter variations with temperature and time. This disadvantage can be improved if the feedback is applied around the complete cascade amplifier. The resulting series-shunt feedback pair is shown in Fig. 11d.

A detailed computer-aided circuit analysis has been made of the series-shunt cascade and the series-shunt feedback pair. The results of the comparison indicate that overall feedback leads to a larger gain desensitivity than local feedback while providing comparable gain and bandwidth.

The basic feedback equation is given by

$$A_V = \frac{a_V}{1 + a_V f_V}$$

where a_V = open-loop voltage gain
f_V = feedback factor
A_V = closed-loop voltage gain

In the limit as $a_V \to \infty$,

$$A_V = \frac{1}{f_V}$$

In Fig. 11d,

$$f_V = \frac{R_E}{R_E + R_F}$$

hence $$\frac{v_o}{v_s} = A_V \simeq \frac{R_E + R_F}{R_E} = 1 + \frac{R_F}{R_E}$$

Experimental Amplifier I

Figure 12a shows the schematic diagram of a series-shunt feedback pair[4] using complementary transistors, whose f_T is about 1 GHz. The amplifier is dc coupled with a 50 Ω termination at the input. The load resistance is also 50 Ω. For a voltage gain of 10, with R_F = 280 Ω, R_E should be 31 Ω. This is obtained from the series combination of D_1 and R_{E1}. The pulse response for the amplifier as obtained from computer-aided analysis is shown in Fig. 12b. Notice the low frequency voltage gain is indeed 10 (actually a little more). The figure also shows the effect of the peaking capacitance, C_6, which is C_E in the schematic diagram. With C_6 = 20 pF, there is negligible overshoot to the transient response and the risetime (10 to 90%) is ~1 ns. The risetime as actually measured on a physical amplifier is about 1.3 ns. The question then arises, why this difference?

Several factors limit the high frequency response of an amplifier, the most important being the f_T of the transistors. However, the frequency response of a wideband pulse amplifier may also be restricted by i) the components used are not ideal and may have a certain amount of parasitic inductance and capacitance associated with them, and ii) the overall physical size of the layout may also introduce parasitic inductance and capacitance into the circuit.

The hybrid fabrication technique[4], using thin film resistors and chip transistors and capacitors mounted on a dielectric substrate, is an attempt to improve the amplifier frequency response through the elimination of some of these parasitic effects. Also using the hybrid technique we can make use of microstrip transmission lines of 50 Ω impedance to extend the signal lines to the base of the input transistor and from the collector of the output transistor.

Another problem with high frequency circuits is the measurement of the transistor parameters at these frequencies. The characteristics of a transistor are commonly described with the h-parameters shown in Fig. 13. Each of these measurements require either a short-circuit at the output or an open-circuit at the input of the transistor. A complete open-circuit is difficult to achieve at high frequencies due to stray capacitances. A short-circuit is easier to achieve, though eventually a frequency is reached where even the self-inductance of the short becomes important.

To overcome these difficulties a set of parameters have been taken from the microwave area. These are the scattering (s) parameters shown in Fig. 14. First used to characterize the travelling wave patterns in a waveguide, they are an extension of transmission line theory.

Now the input and output impedance of a transistor are complex quantities which are a function of frequency. However, a plot of the real and imaginary parts of these quantities is required to give some meaning to these impedances. This is readily done with another idea taken from the microwave area--the Smith chart. The typical input and output characteristics of a high frequency transistor are shown plotted on a Smith chart in Fig. 15. The forward and reverse transfer characteristic are better plotted on a polar graph, which displays the magnitude and phase angle of these coefficients as a function of frequency.

The use of s-parameters in the design of microwave amplifiers has been well documented.[5] However, the bandpass of these amplifiers are generally only of the order of one octave (viz, 1 to 2 GHz). While the use of s-parameter has afforded us a way of characterizing high frequency transistors, their use in the design of truly wideband amplifiers (dc - 1 GHZ) is not so readily obvious. This is more easily handled with the familiar hybrid-π circuit model for the transistor. Also suitable computer-aided analysis programs, which are necessary in the design of hybrid ICs, make use of the hybrid-π model. Accordingly a computer program has been written which, given a set of s-parameter data for a transistor, automatically determines the components of the hybrid-π model to whatever level of complexity is desired.[6]

Experimental Amplifier II

The circuit diagram of a series-shunt feedback pair using microwave transistors is shown in Fig. 16a.[6] This circuit was fabricated as a hybrid IC on a 1" x 1" sapphire substrate. The physical layout is shown in Fig. 16b. The circuit model which was used in the computer-aided analysis is shown in Fig. 17. The component values of the model for the transistor were obtained from s-parameter measurements of the chip transistors. The model also includes parasitic effects, such as the inductance of the bonding leads and the capacitance of the thin film resistors to the ground plane.

The s-parameter results of the computer analysis are compared with the experimentally determined results in Fig. 18. For the forward insertion gain (s_{21}), Fig. 18a shows a ±1 dB variation about the nominal gain of 20 dB. The cut-off frequency (f_h) is in excess of 1 GHz. Of interest in any high-speed pulse system is the input reflection coefficient. This is plotted as s_{11} in Fig. 18b. In both cases, of s_{21} and s_{11}, note the excellent agreement between theory and practice.

The small-signal step response of the series-shunt feedback pair is shown in Fig. 19. With a step input (t_r = 60 ps), the amplifier shows of voltage gain of 10 and a output risetime of ~400 ps. This is in good agreement with the computer-aided results of ~370 ps and overshoot of ~10% obtained from the model of Fig. 17 being driven by a pulse with a linear front edge of 60 ps risetime.

Further Developments

A further refinement to broadbanding pulse amplifiers is the use of series and shunt peaking. The effectiveness of such methods dates back many years.[7] A hybrid IC 3-stage amplifier which makes use of local series and shunt feedback, as well as series and shunt peaking with thin film spiral inductors has recently been described.[8] The overall gain of the amplifier is 26 dB with a frequency response from 0.1 to 1.3 GHz. In another development,[9] the parasitics of the circuit are ingeniously incorporated into the peaking network of a monolithic IC broadband amplifier to yield a nominal gain of 9 dB and a pulse risetime of 330 ps.

CONCLUSION

If the sole interest is to accurately determine the amplitude of a pulse, even a nanosecond pulse, then it is necessary to maximize the S/N ratio. To do this, the bandpass frequency of the amplifier must be restricted. There will be an optimum pulse shaping network, or networks, to achieve this.

In a pulse timing application, where again low noise is also important, unless the detector and amplifier can be integrated then the series-shunt cascade feedback amplifier configuration is indicated. With increasing upper cut-off frequencies the time delay in a feedback amplifier pair becomes prohibitive.

ACKNOWLEDGEMENT

I would like to thank Tom Shimizu for his valuable assistance in this work.

REFERENCES

1. Ghausi, M. S., Principles and Design of Linear Active Networks, McGraw-Hill Inc., New York (1965).

2. Cherry, E. M. and Hooper, D. E., Amplifying Devices and Low-Pass Amplifier Design, Wiley and Sons Inc., New York (1968).

3. Goulding, F. S., "A Survey of the Applications and Limitations of Various Types of Detectors in Radiation Energy Measurement", IEEE Trans. Nucl. Sci. NS-11, No. 3, 177 (1964).

4. Jackson, H. G. and Mattis, J. A., "A Direct-Coupled Hybrid IC Amplifier with 1 ns Risetime", IEEE J. Solid-State Circuits, SC-4, No. 2, 86 (1969).

5. "S-Parameter Design", Hewlett-Packard Application Note #154, April 1972.

6. Wilson, R. S., "The Use of Scattering Parameters in the Design of Amplifiers with Subnanosecond Risetime", Lawrence Berkeley Laboratory Report LBL-772, February 1972.

7. Valley, G. E. and Wallman, H., Vacuum Tube Amplifiers, McGraw-Hill Inc., New York (1948).

8. "A 0.1 to 1.3 GHz Amplifier", Hewlett-Packard Journal, March 1973.

9. Addis, J., "Three Technologies on One Chip Make a Broadband Amplifier", Electronics, Vol. 45, No. 12, 103 (1972).

ANNOTATED BIBLIOGRAPHY

The following books are of interest:

M. S. Ghausi, "Principles and Design of Linear Active Circuits", McGraw-Hill, Inc., New York (1965).
A textbook on the principles and the techniques used in the analysis and design of linear active circuits. The emphasis is on transistor circuits, but vacuum tubes are also included. There is a good coverage of wideband cascaded stages as well as feedback stages.

E. M. Cherry and D. E. Hooper, "Amplifying Devices and Low-Pass Amplifier Design", Wiley and Sons, Inc., New York (1968).
A general textbook on the subject, covering the characteristics of vacuum tubes, bipolar and field-effect transistors and their application in small signal as well as large signal amplifiers. Also covered are noise, feedback (both single stage and multistage) and wideband amplifier design.

W. Meiling and F. Stary, "Nanosecond Pulse Techniques" Gordon and Breach Science Publishers, New York (1968).
A review of nanosecond pulse measuring techniques as applied in nuclear science. Subject matter includes radiation detectors, electronic circuits (amplifiers, time analyzers, logic circuits and scaling circuits) and test apparatus. The book has an extensive bibliography.

Some papers on the general subject of the design of wideband amplifiers:

E. M. Cherry and D. E. Hooper, "The Design of Wideband Transistor Feedback Amplifiers", Proc. IEE (London) Vol. 110, 375 (1963).
An early but good study of the subject. The equations for both gain and bandwidth of the series-shunt cascade are developed in detail, but multi-stage feedback loops are also covered.

J. E. Soloman and G. R. Wilson, "A Highly Desensitized Wideband Monolithic Amplifier", IEEE J. Solid-State Circuits, SC-1, 19 (1966).
A detailed analysis is made of the use of series-series feedback in a broadband integrated circuit amplifier. While the particular interest of the authors is to a monolithic IC amplifier, there is general information which should be useful.

B. A. Wooley, "Design Optimization of Integrated Broadband Amplifiers", Ph.D. Thesis, University of California, Berkeley, 1970.
A detailed study is made of a number of basic feedback configurations to obtain a wideband amplifier. By the extensive use of computer-aided analysis the parameters of each circuit are optimized for a given gain and maximum bandwidth.

Some technical papers on nanosecond amplifiers:

C. J. Rush, Rev. Sci. Inst., Vol. 35, No. 2, 149 (1964).
The basic current amplifier stage is a shunt-series feedback pair with an input npn common-base transistor followed by a pnp emitter-follower. The npn (2N709) has an f_T of 800 MHz and the pnp (2N976) an f_T of 900 MHz. The stage gain is 4.6 with a risetime of 1.25 ns. Five stages are cascaded for an overall gain of 1580 and a risetime of 3.05 ns. With 50 Ω at the input, the equivalent input noise current is 0.32 μA. An analysis of the feedback pair is included.

J. S. Lunsford, Rev. Sci. Inst., Vol. 35, No. 11, 1483 (1964).
A basic current amplifier where a common-base transistor (2N918) with shunt peaking in the collector, drives a series feedback transistor (2N918) with capacitive peaking in the emitter. Six stages are cascaded for a current gain of 100 and a risetime of 1 ns. The maximum output is 1 V in 50 Ω. The equivalent noise at the input is 70 μV rms.

M. A. Schapper, Nucl. Instr. and Methods, Vol. 27, 172 (1964).
A voltage amplifier with series-shunt feedback, using complementary transistors (2N709 and 2N976). The voltage gain is 10. With an output of 5 V into 125 Ω, the risetime is 2 ns. The noise, referred to the input, is 76 μV rms.

H. G. Jackson, Nucl. Instr. and Methods, Vol. 33, 161 (1965).
A series-shunt feedback pair using two 2N2857 transistors. The amplifier is dc coupled, with a voltage gain of 10; 50 Ω in and 50 Ω out. Output risetime is 1 ns, with a maximum amplitude of 1 V. The equivalent input noise is 50 μV rms.

M. Goyot, et al, Nucl. Instr. and Methods, Vol. 46, 149 (1967).
A common-base transistor (2N3284) with shunt peaking in the collector, drives a series feedback transistor (NS910) with capacitive peaking at the emitter. Shunt-shunt feedback is also applied between the emitter of the first transistor and the collector of the second transistor. A cascade of three such stages has a gain of 10, and a risetime of 1.2 ns for a 1 V output pulse into 50 Ω. The connection of the output of the first stage to the input of the second forms a cascode circuit. An analysis of the frequency compensation of the cascode circuit is included.

P. F. Manfredi and A. Rimini, Nucl. Instr. and Methods, Vol. 49, 71 (1967).
A basic shunt-shunt feedback pair with a common-emitter transistor at the input driving an emitter-follower. Bootstrapping the output of the second transistor back to the first transistor decreases the "Miller effect" at the collector of the common-emitter transistor. The two npn transistors have an f_T of about 1.2 GHz. The amplifier gain is 10 with a risetime of 1.2 ns for negative input pulses and 1.9 ns for positive input pulses.

A. Tojo, Nucl. Instr. and Methods, Vol. 50, 45 (1967).
A three-stage current amplifier with a gain of 50 and a risetime of 3.2 ns. The basic amplifier consists of two transistors. A current signal from the emitter of a pnp transistor, with shunt feedback from the collector to the input at the base, connects to the emitter of a npn common-base transistor. The low impedance at the input of the second stage provides the load for the output, at the collector of the first stage. The transistors used have an f_T of about 550 MHz. A detailed analysis of the basic amplifier is included.

FIGURE CAPTIONS

Fig. 1. Block diagram of a simple high-energy nuclear physics instrumentation system used in angular correlation studies.

Fig. 2. Block diagram of the instrumentation required for a simple time-of-flight experiment.

Fig. 3. Block diagram for nuclear particle energy determination.

Fig. 4. Thermal noise in a resistor (a) is represented in (b) as a voltage source in series with a noiseless resistor and in (c) as a current source in parallel with a noiseless resistor.

Fig. 5. a) Simple series circuit consisting of a battery, a diode and a resistor.

b) Circuit model of circuit in (a) including sources for shot noise and thermal noise.

Fig. 6. Noise in the amplifier of (a) is combined and referred to the input of a noiseless amplifier as in (b).

Fig. 7. Main sources of noise in a bipolar junction transistor are included in this small-signal hybrid-π model for the device.

Fig. 8. Circuit model of a field effect transistor including the noise sources.

Fig. 9. Equivalent input noise voltage of an amplifier as a function of equal differentiating and integrating time constants.

Fig. 10. Typical gain-frequency response of a high frequency transistor.

Fig. 11. Transistor feedback configurations:

a) Series feedback in a single transistor.

b) Shunt feedback in a single transistor.

c) The series-shunt cascade.

d) The series-shunt feedback pair.

Fig. 12. a) Schematic diagram of series-shunt feedback amplifier pair.

b) Pulse response of the amplifier as determined by computer-aided analysis.

Fig. 13. The common description of the small-signal characteristics of a transistor (a two port) with the h-parameters.

Fig. 14. Description of the s-parameters, used to characterize microwave transistors.

Fig. 15. Typical s-parameter characteristics of a microwave transistor. (Courtesy of Hewlett-Packard.)

Fig. 16. a) Circuit diagram of series-shunt feedback pair used in hybrid IC amplifier.

b) Physical layout on 1" x 1" substrate of hybrid IC amplifier.

Fig. 17. Circuit model used in computer-aided analysis of the hybrid IC amplifier.

Fig. 18. S-parameter measurements of the hybrid IC amplifier:

a) Forward insertion gain (s_{21}).

b) Input reflection coefficient (s_{11}).

Fig. 19. Small-signal step response of the hybrid IC amplifier.

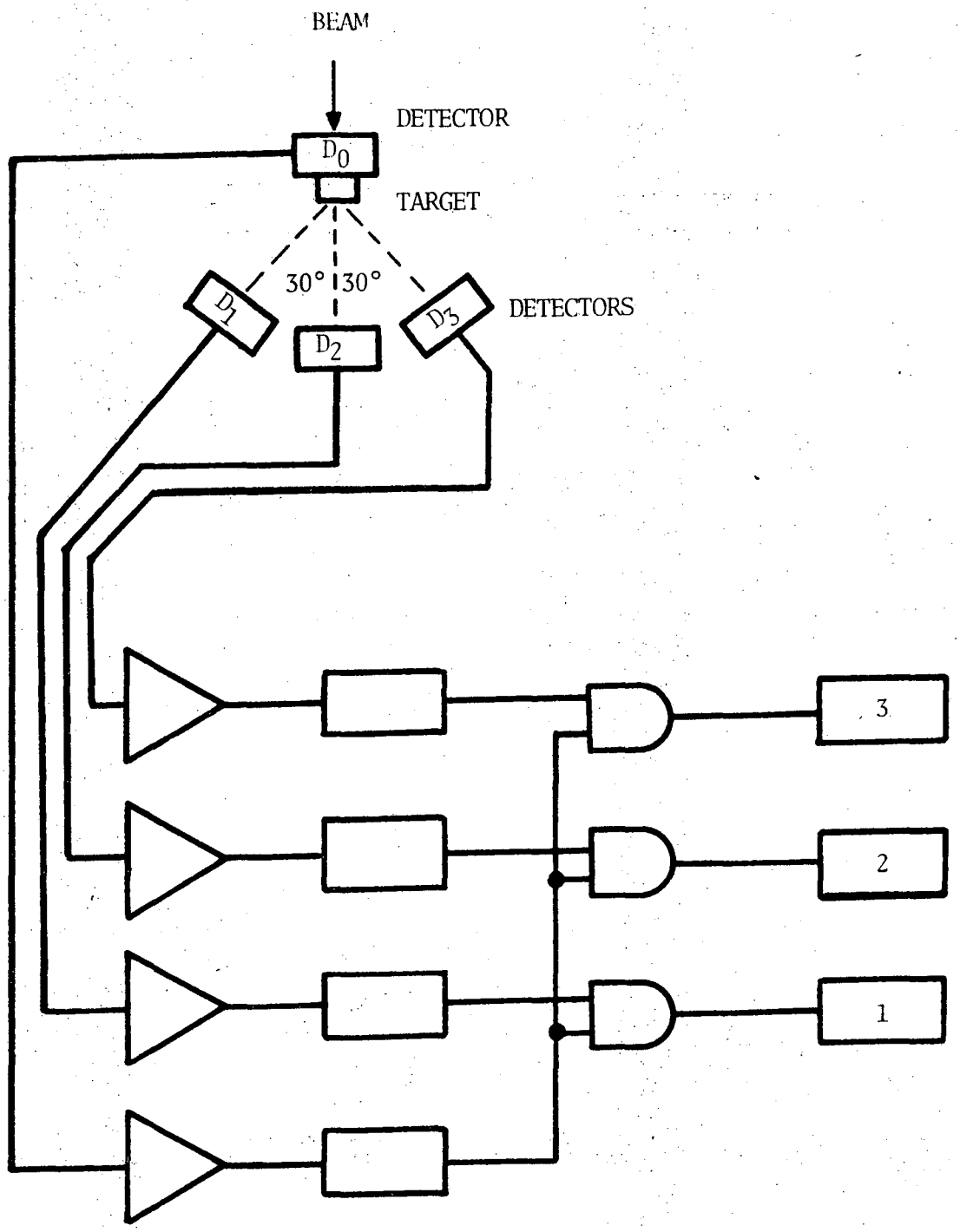

XBL 737-893

Fig. 1

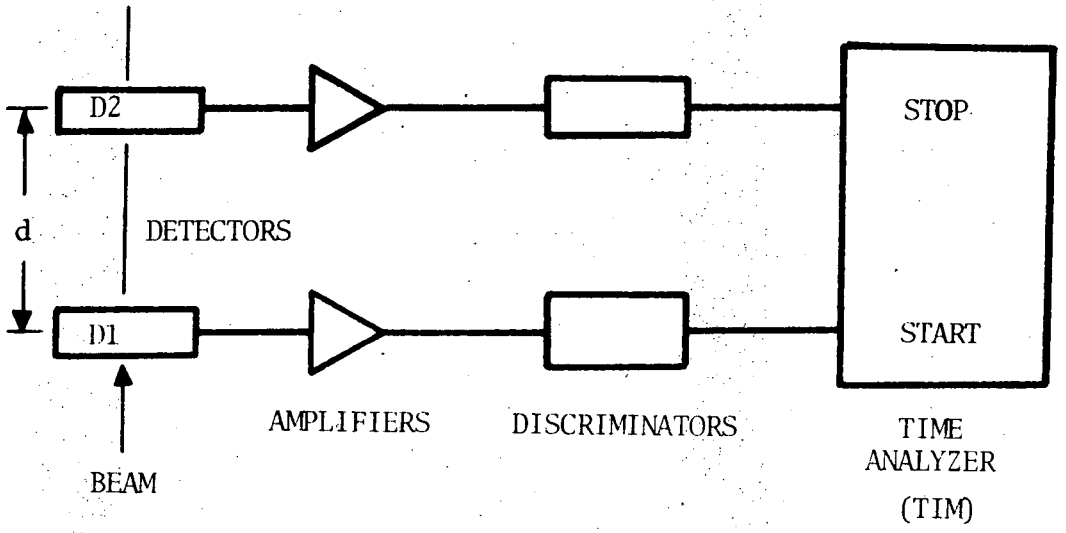

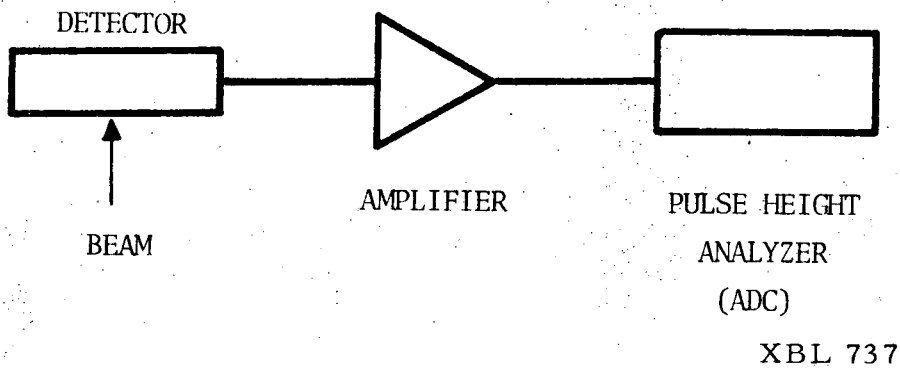

XBL 737-894

Fig. 2

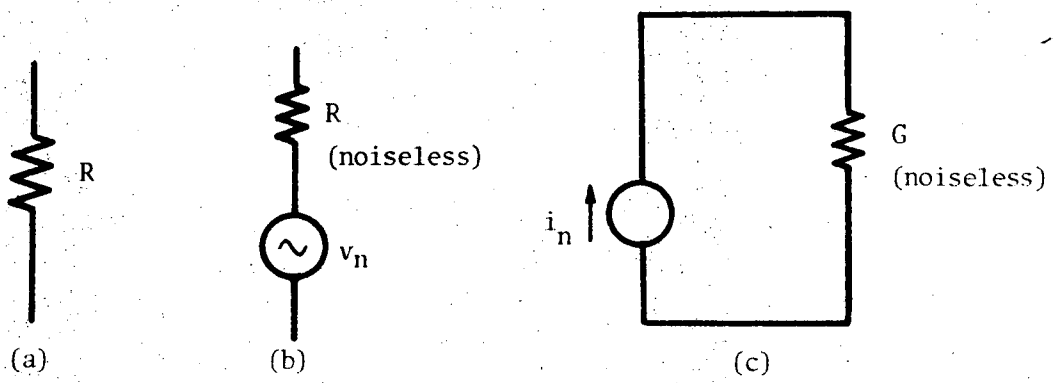
R
(a)
R
(noiseless)
v_n
(b)
i_n
G
(noiseless)
(c)

Fig. 4

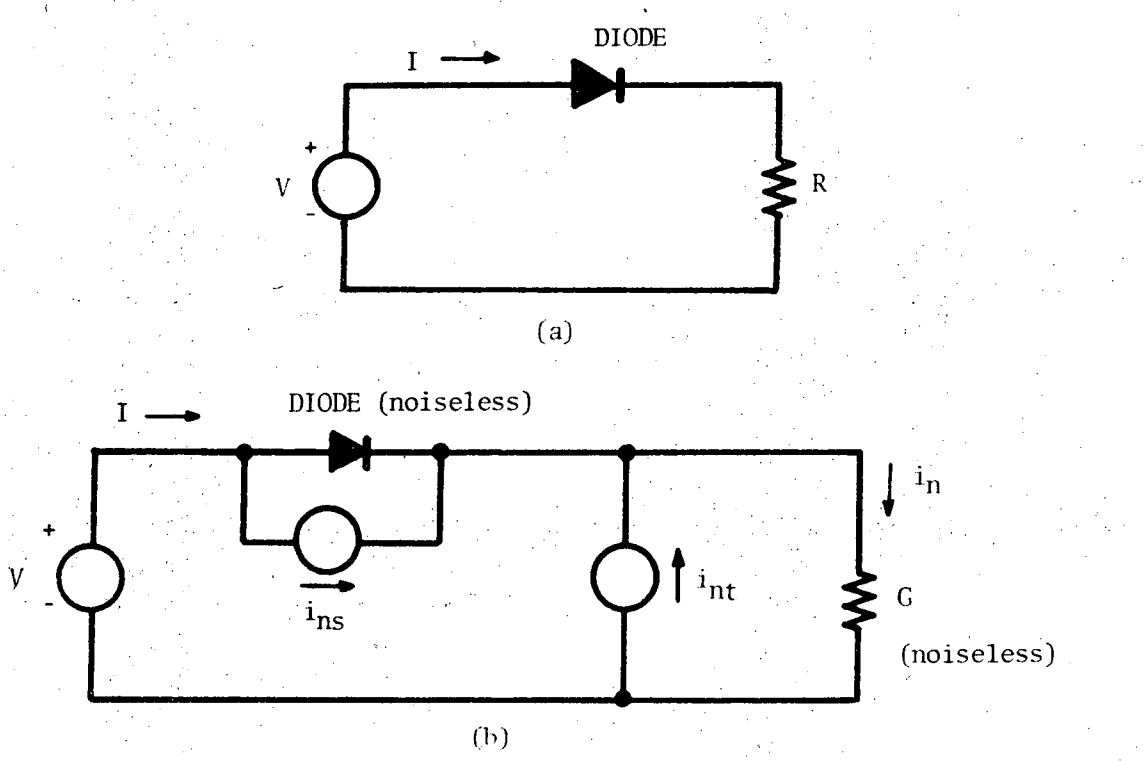
I
DIODE
V
R
(a)
I
DIODE (noiseless)
V
i_{ns}
i_{nt}
i_n
G
(noiseless)
(b)
XBL 737-895

Fig. 5

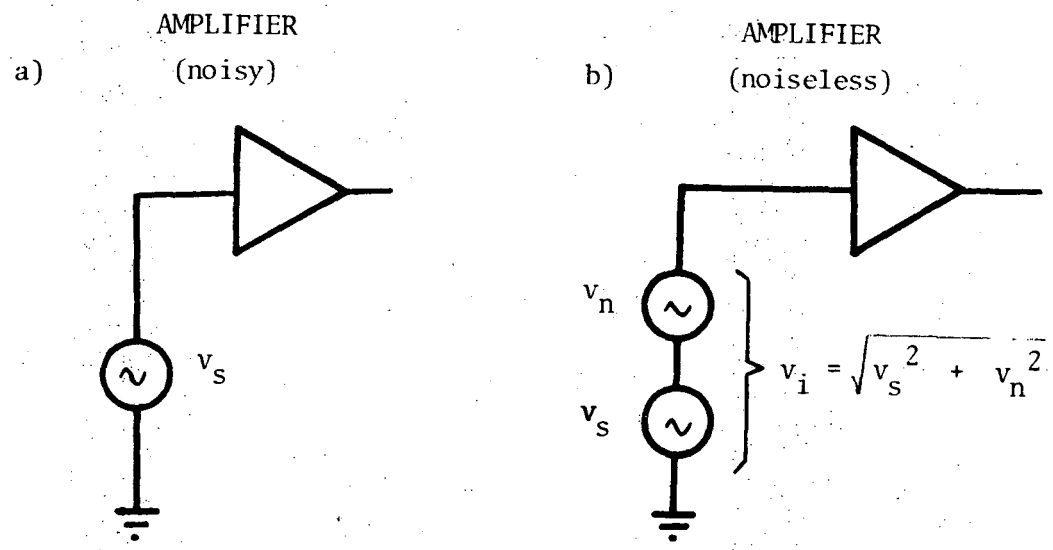

Fig. 6

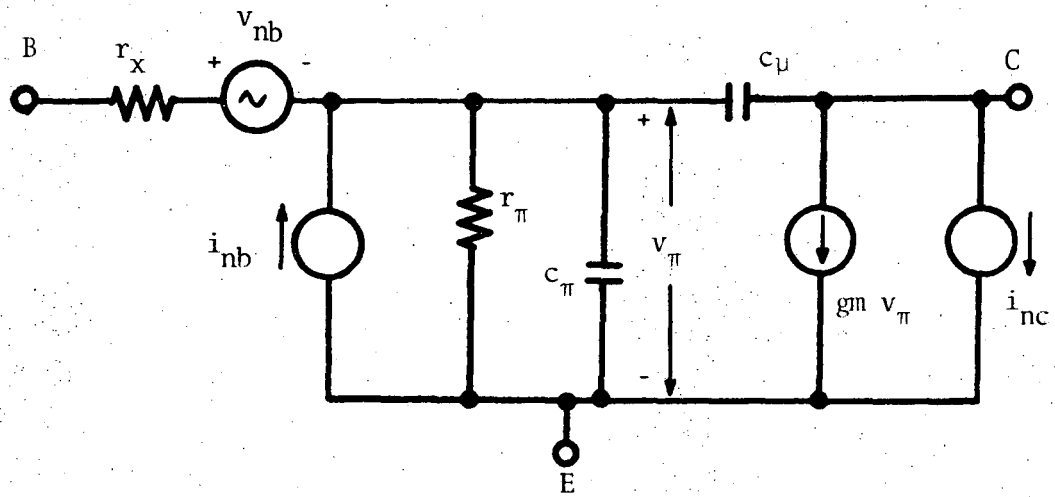

XBL 737-896

Fig. 7

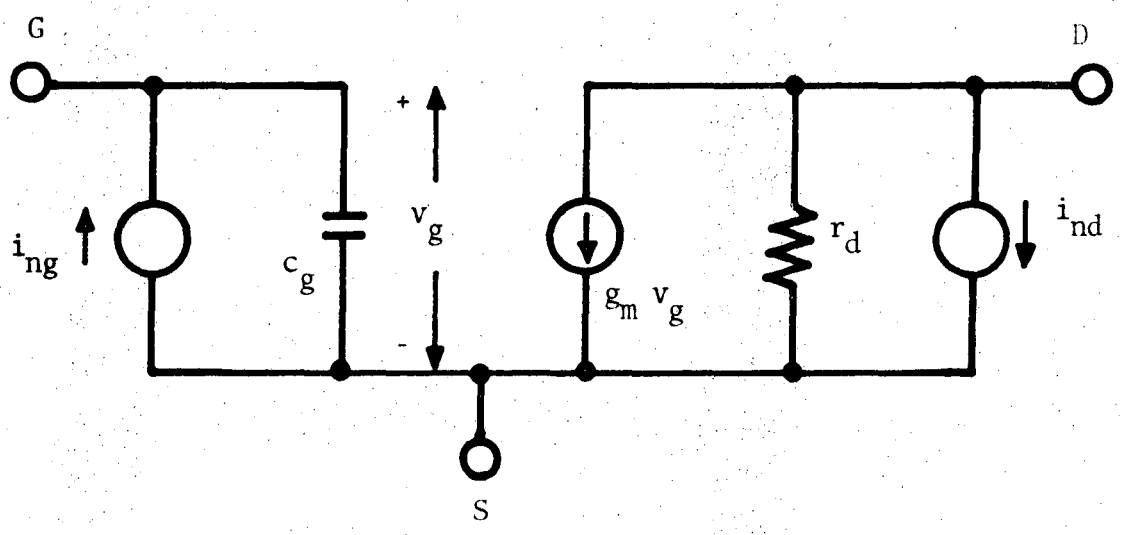

XBL 737-897

Fig. 8

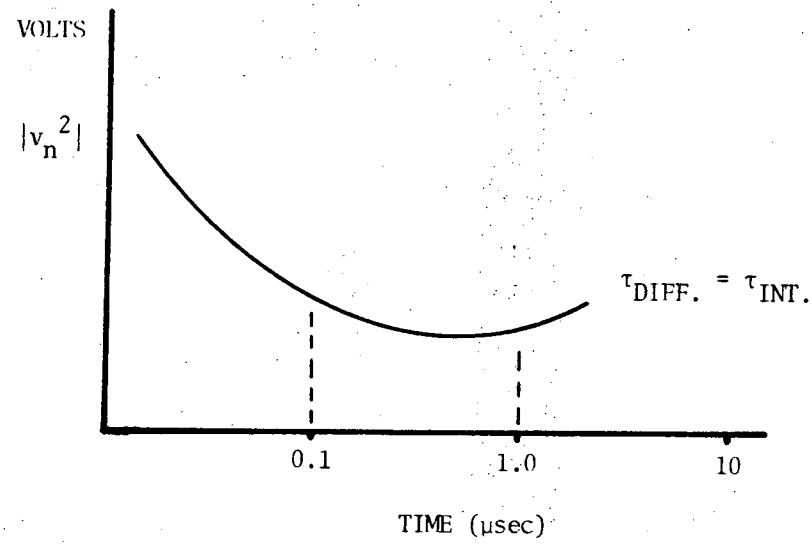
VOLTS
$|v_n^2|$
$\tau_{DIFF.} = \tau_{INT.}$
0.1
1.0
10
TIME (μsec)

Fig. 9

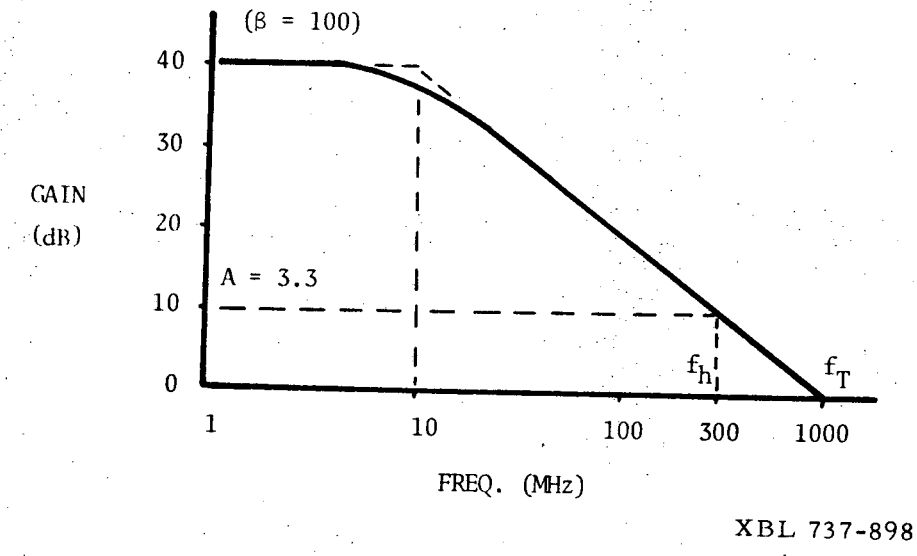
(β = 100)
40
30
20
10
0
GAIN
(dB)
A = 3.3
f_h
f_T
1
10
100
300
1000
FREQ. (MHz)
XBL 737-898

Fig. 10

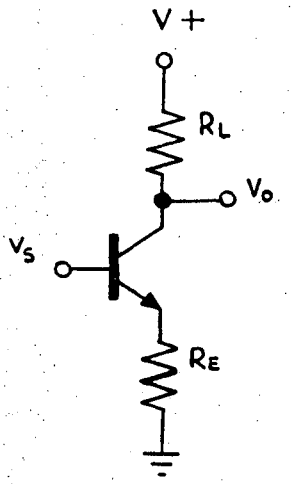

(a) SERIES FEEDBACK

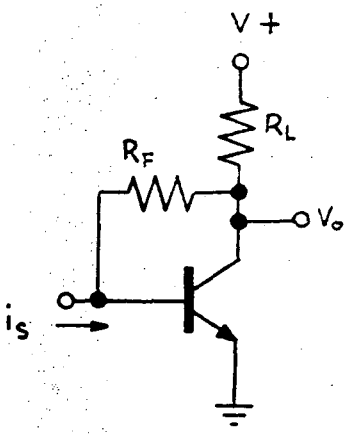

(b) SHUNT FEEDBACK

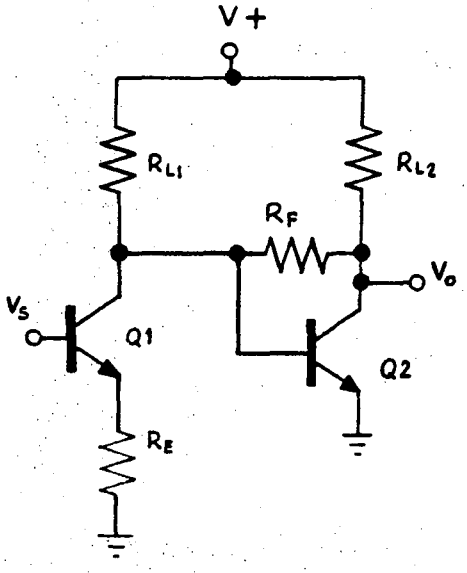

(c) SERIES SHUNT CASCADE

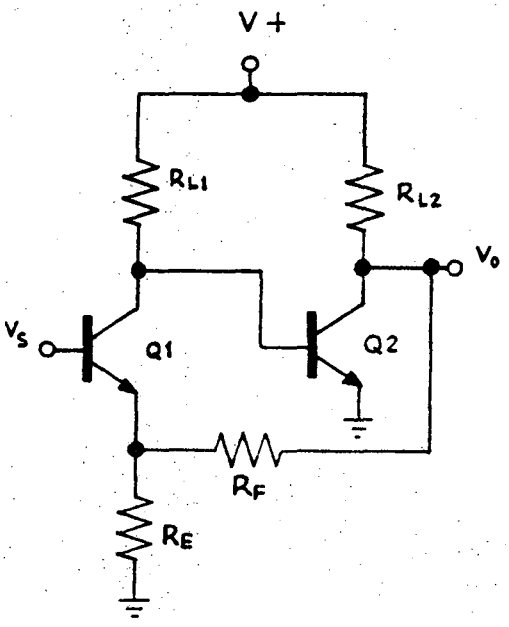

(d) SERIES SHUNT FEEDBACK PAIR

XBL 737-899

Fig. 11

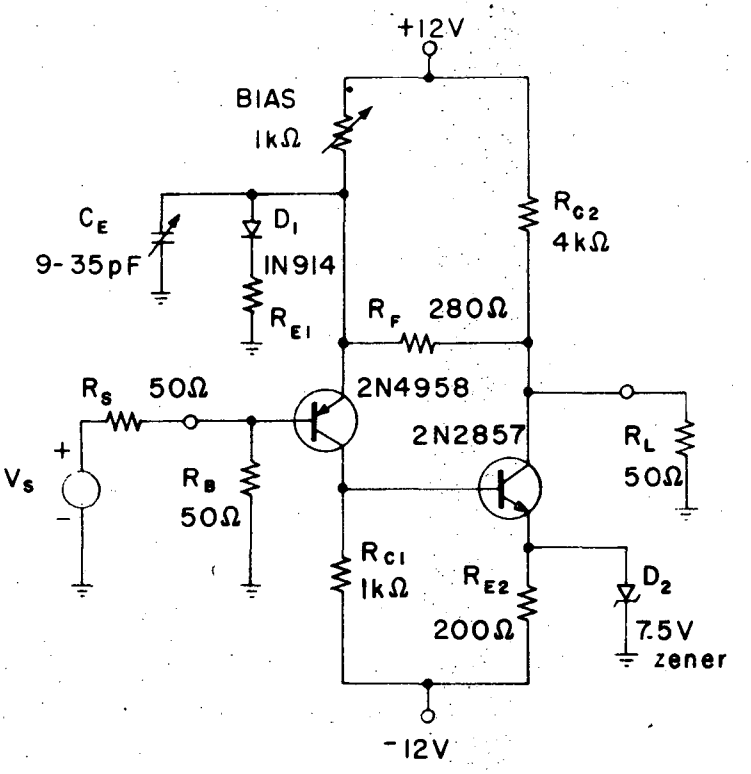

(a)

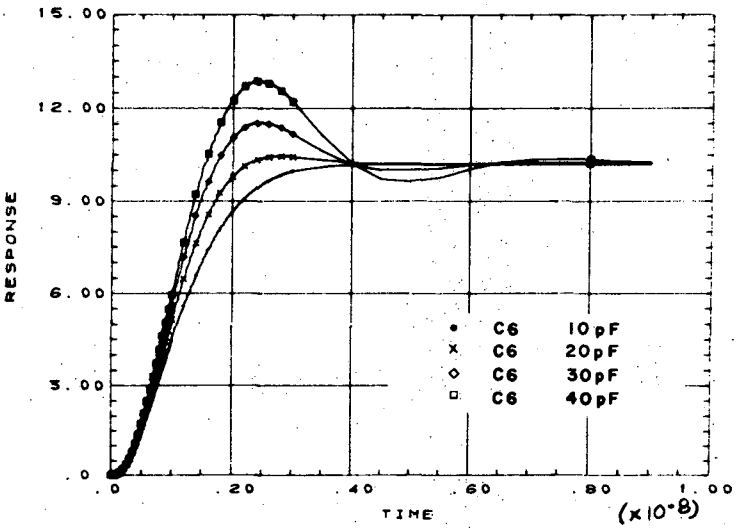

(b)

XBL 737-901

Fig. 12

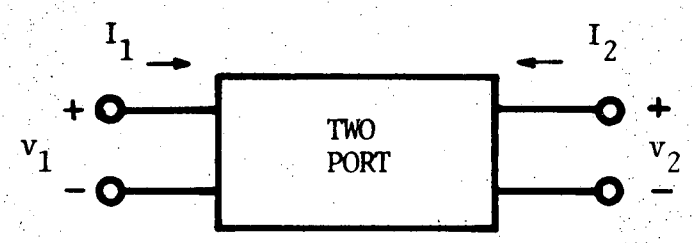

H - PARAMETERS

$$V_1 = h_{11} I_1 + h_{12} V_2$$

$$I_2 = h_{21} I_1 + h_{22} V_2$$

$$h_{11} = \left.\frac{V_1}{I_1}\right|_{V_2 = 0} = \text{Input impedance with a short circuit at the output}$$

$$h_{22} = \left.\frac{I_2}{V_2}\right|_{I_1 = 0} = \text{Output admittance with a open circuit at the input}$$

$$h_{21} = \left.\frac{I_2}{I_1}\right|_{V_2 = 0} = \text{Forward current gain with a short circuit at the output}$$

$$h_{12} = \left.\frac{V_1}{V_2}\right|_{I_1 = 0} = \text{Reverse voltage gain with a open circuit at the input}$$

XBL 737-891

Fig. 13

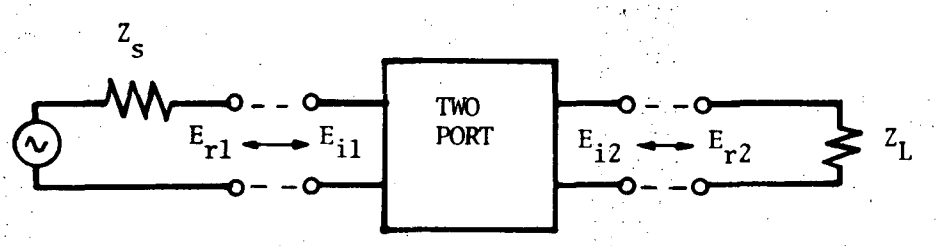

S - PARAMETERS

$$b_1 = s_{11}\, a_1 + s_{12}\, a_2$$

$$b_2 = s_{21}\, a_1 + s_{22}\, a_2$$

$$a_1 = \frac{E_{i1}}{\sqrt{Z_o}} \qquad b_1 = \frac{E_{r1}}{\sqrt{Z_o}}$$

$$a_2 = \frac{E_{i2}}{\sqrt{Z_o}} \qquad b_2 = \frac{E_{r2}}{\sqrt{Z_o}}$$

$s_{11} = \left.\frac{b_1}{a_1}\right|_{a_2 = 0}$ = Input reflection coefficient with the output port terminated by a matched load ($Z_L = Z_o$ sets $a_2 = 0$)

$s_{22} = \left.\frac{b_2}{a_2}\right|_{a_1 = 0}$ = Output reflection coefficient with the input port terminated by a matched load ($Z_s = Z_o$ sets $a_1 = 0$)

$s_{21} = \left.\frac{b_2}{a_1}\right|_{a_2 = 0}$ = Forward insertion gain (matched load)

$s_{12} = \left.\frac{b_1}{a_2}\right|_{a_1 = 0}$ = Reverse insertion gain (matched load)

XBL 737-890

Fig. 14

TYPICAL CHARACTERISTICS

SMALL-SIGNAL COMMON-EMITTER S PARAMETERS

► V_{CE} = +15 V, I_C = +15 mA, $Z_G = Z_L$ = 50 ohms + j0, T_A = 25°C

INPUT IMPEDANCE and INPUT REFLECTION COEFFICIENT, S_{11e}

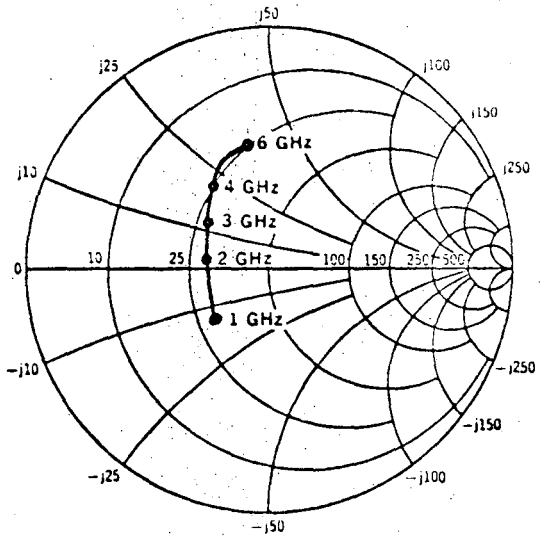

Coordinates in ohms

OUTPUT IMPEDANCE and OUTPUT REFLECTION COEFFICIENT, S_{22e}

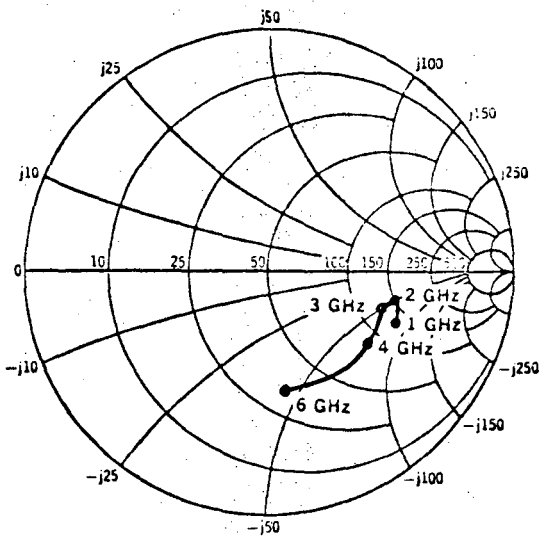

Coordinates in ohms

FORWARD TRANSFER COEFFICIENT, S_{21e}

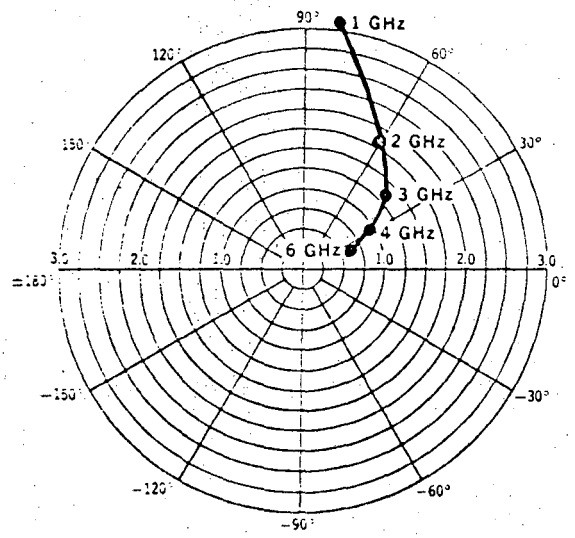

REVERSE TRANSFER COEFFICIENT, S_{12e}

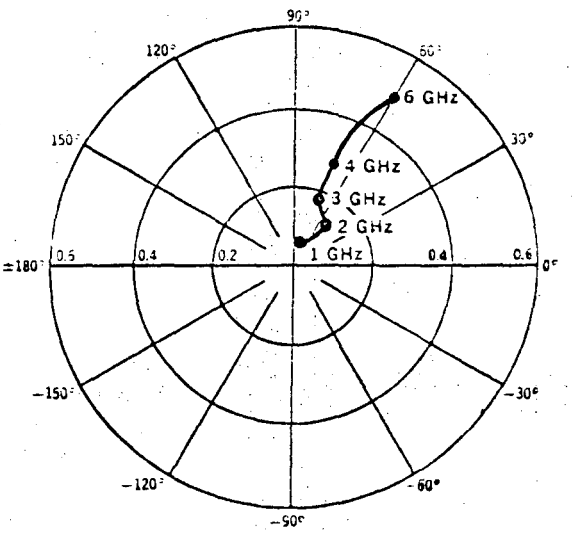

Note: Data includes effects of 0.7 mil bonding wire 20 to 30 mils long.

XBL 737-892

Fig. 15

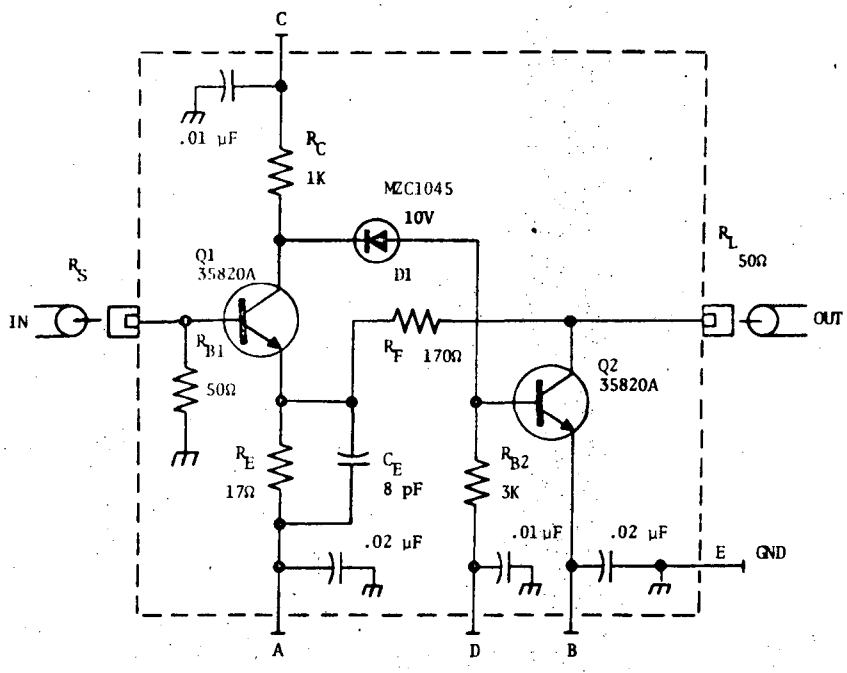

(a)

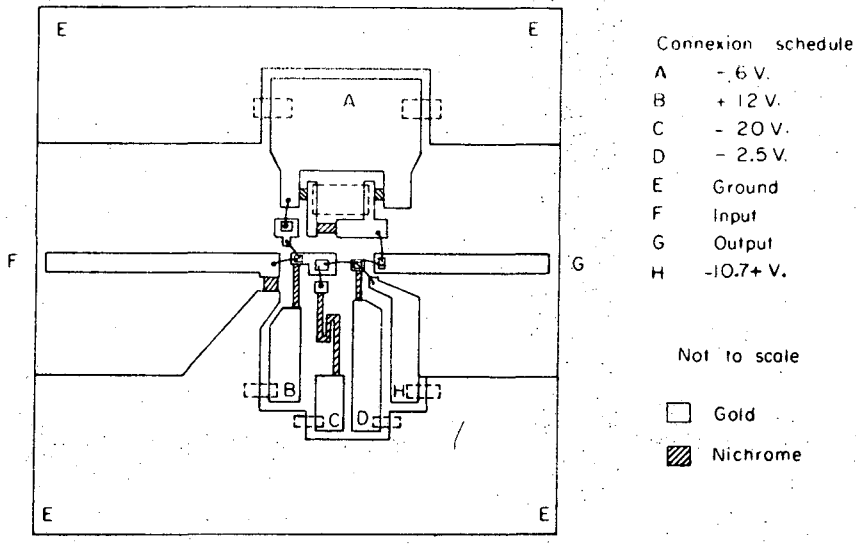

(b)

XBL 737-900

Fig. 16

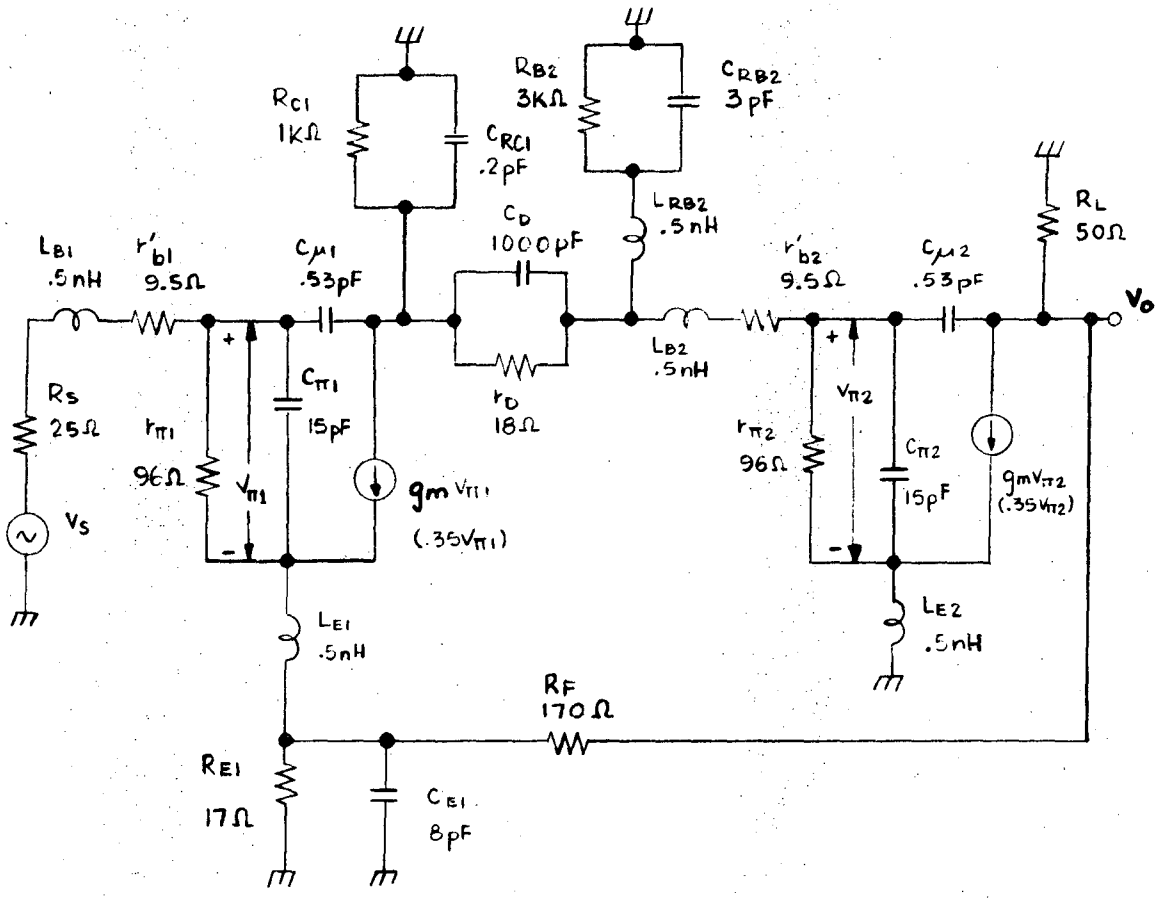

XBL 737-889

Fig. 17

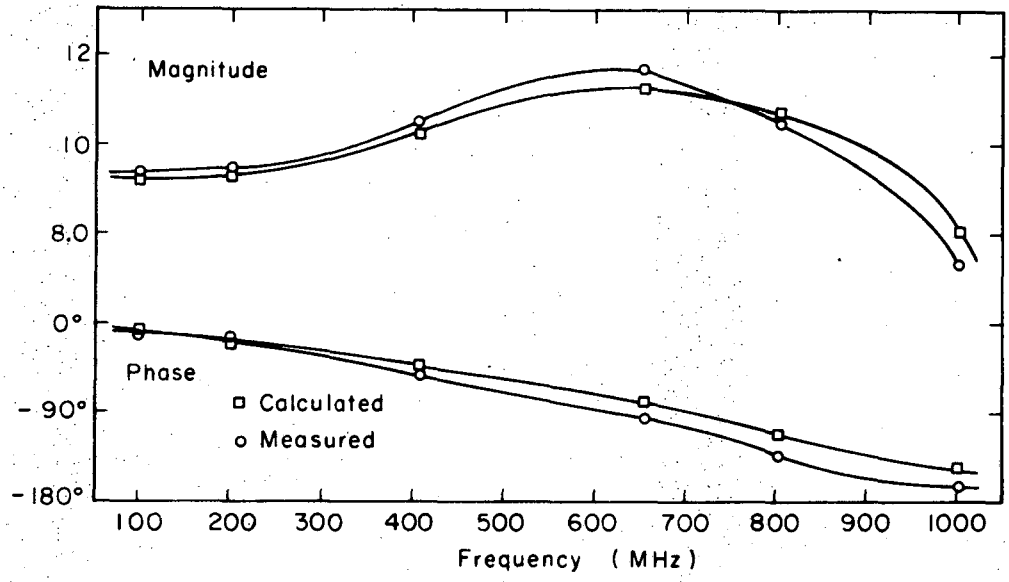

(a)

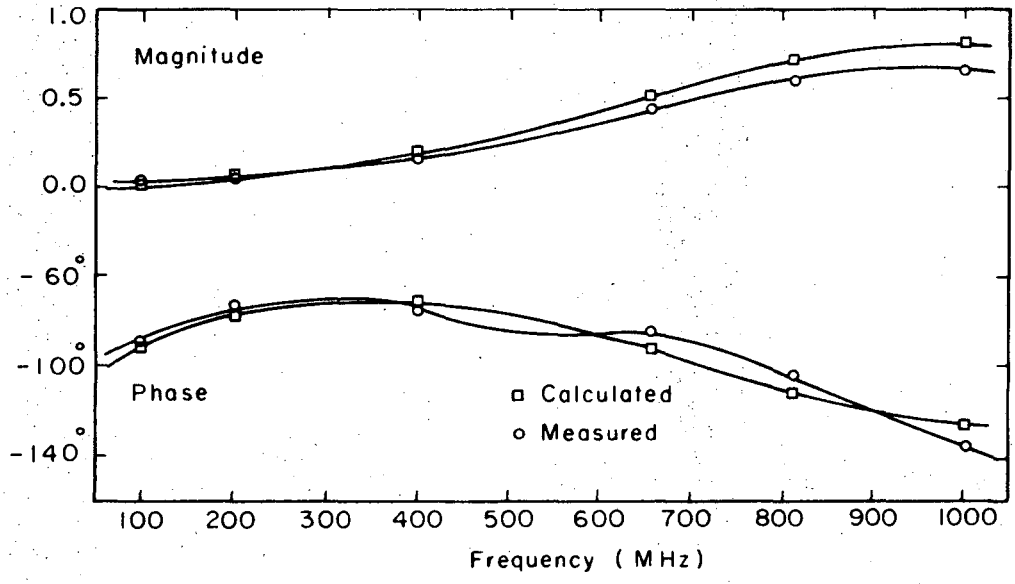

(b)

XBL 737-888

Fig. 18

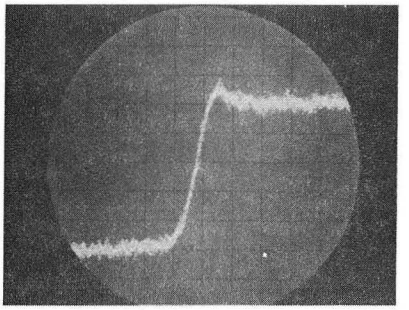

FIG. 5-11a

INPUT WAVEFORM
50 ps/div.
2 mV/div.

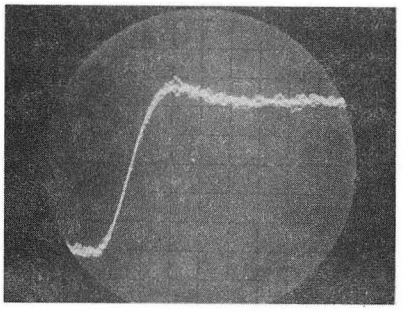

FIG. 5-11b

OUTPUT WAVEFORM VIA
20 dB ATTEN.
400 ps/div.
2 mV/div.

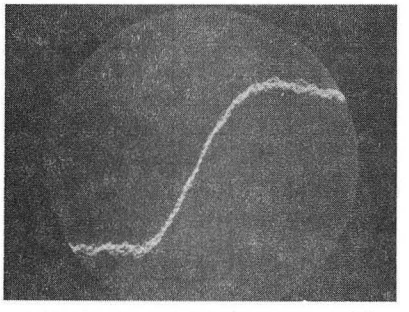

FIG. 5-11c

OUTPUT WAVEFORM VIA
20 dB ATTEN.
200 ps/div.
2 mV/div.

XBB 721-397

FIG. -19- SMALL-SIGNAL STEP RESPONSE
OF THE SERIES-SHUNT PAIR

TECHNICAL INFORMATION DIVISION
LAWRENCE BERKELEY LABORATORY
UNIVERSITY OF CALIFORNIA
BERKELEY, CALIFORNIA 94720